Electrical Power and Energy Systems 80 (2016) 312–324

Contents lists available at ScienceDirect

Electrical Power and Energy Systems

journal homepage: www.elsevier.com/locate/ijepes

Ultra high speed deterministic algorithm for transmission lines disturbance identification based on principal component analysis and Euclidean norm

J.A. Morales [a,b,*], E. Orduña [a], C. Rehtanz [c], R.J. Cabral [d], A.S. Bretas [d]

[a] Instituto de Energía Eléctrica, Universidad Nacional de San Juan, Av. Lib. Gral. San Martín Oeste 1109 (J5400ARL), San Juan, Argentina
[b] Carrera de Ingeniería Mecatrónica, Universidad Politécnica Salesiana, Calle Vieja 12-30 y Elia Liut, 010150 Cuenca, Ecuador
[c] Institute of Energy Systems, Energy Efficiency and Energy Economics of TU Dortmund University, Emil-Figge-Straße 70, 44227 Dortmund, Germany
[d] Electrical Engineering Department, Federal University of Rio Grande do Sul, Av. Osvaldo Aranha, 103 – Room 116, Porto Alegre, Rio Grande do Sul 90035-190, Brazil

ARTICLE INFO

Article history:
Received 17 January 2014
Received in revised form 14 January 2016
Accepted 27 January 2016

Keywords:
Deterministic algorithm
Undesirable conditions
Ellipsoidal pattern
Euclidean norm

ABSTRACT

Protection devices are designed to provide high sensitivity to transients produced by undesirable conditions like lightning stroke, avoiding their operation under all tolerable events like switching operations. The problem of incorrect operation due to transient phenomena can be handled by two means, one is to allow the transients and provide additional logics in the relay, other means is to damp the oscillation from source side. Protection relays' not always must trip or send a trip signal and sometimes, only an alarm is necessary. In this context, this research presents a fast and reliable formulation for transmission lines (TLs) switching operations and lightning strokes detection and identification.

The proposed methodology is based on Principal Component Analysis (PCA) and Euclidean Norm (EN); by using PCA it is possible to determine that normal operation signals describe a very well defined Ellipsoidal Pattern (EP). In this manner, by calculating the Euclidean Norm (EN) among Principal Components (PCs) for each sample and the origin of the reference Ellipsoidal Pattern, switching operations and lightning strokes are detected and identified. Test results show that the proposed algorithm presents high success on phenomena detection and identification, presenting a high potential for online applications.

Introduction

Protection relays must distinguish correctly abnormal conditions from normal operating conditions. Nevertheless, both phenomena can generate over-voltage waves, specially produced by atmospheric discharges or switching operations [1].

Faults mostly occur in TLs, still the highest percentage of power outages are especially due to lightning strokes [2–9], which are considered as the most intolerable phenomenon for the TLs performance.

On the other hand, switching operations of TLs, loads, transformers and others can generate travelling waves, which are often considered negligible [10]. However, it is well accepted that these signals can produce mal-operation of protection devices, being a possible cause not only of unnecessary relay actuations, but also of transmission line disconnections [11–13], affecting potentially the stability and integrity of Electric Power Systems (EPS) [14]. Thus, in order to avoid these drawbacks, protection relays must send correctly the trip order [15].

Protection relays can produce tripping or alarm signals. This decision making is usually done through a deterministic approach [16], which compares estimated with fixed or adjusted threshold values. Hence, by using these values, different conditions can be identified.

On the other hand, from the bibliographic review, some researchers have proposed different approaches to make the event identification, especially focused to Power Quality (PQ) problems and the disturbance classification [17–19]. These and other publications have proposed the use of several signal processing techniques as Fourier Transform (FT), Wavelet Transform (WT), Artificial Neural Network (ANN), Support Vector Machine (SVM), Park's transformation and S-transform [20–42] to make the event identification. As regards to WT, it has been widely employed for PQ problems, but their performance depends on the chosen mother wavelet type [43,44]. On the other hand, FT is not the most

* Corresponding author at: Carrera de Ingeniería Mecatrónica, Universidad Politécnica Salesiana, Calle Vieja 12-30 y Elia Liut, 010150 Cuenca, Ecuador.

http://dx.doi.org/10.1016/j.ijepes.2016.01.043
0142-0615/

adequate technique to analyze non-stationary signals; where their minimum operation time range to analyze switching operations and lightning strokes is from 1 to 3 cycles, respectively [45]. By using the Short-Time Fourier Transform (STF) and S-transform (ST), an operation time of 1/2 cycle can be obtained. However, these proved to be useful to analyze specific conditions different to lightning strokes, where high frequencies are not considered [15].

In this context, it is imperative to develop new methodologies for switching operations and lightning strokes detection and identification. Unlike those previous pieces of research, in this paper, Principal Component Analysis (PCA) is used to develop a novel detection-identification methodology. The algorithm to make the detection of transient signals on TLs is based on the Ellipsoidal Pattern (EP). Accordingly, in normal operation conditions, their signals show trajectories along of the EP. On the contrary, signals during conditions different to normal operation are localized outside of the EP. As regards the identification algorithm, it is based on the Euclidean Norm (EN) among PCs for each sample and the origin of the reference Ellipsoidal Pattern. This work shows that different patterns corresponding to normal conditions, switching operations, lightning strokes and others can be correctly extracted and identified through the EN and EP analysis.

The remaining of this paper is presented as follows: Section 'Principal component analysis' presents the mathematical tool employed in this work. Section 'Electric power system' presents the power system simulated. The proposed methodology is presented in Sections 'Proposed methodology' and 'Performance evaluation'. Section 'Flow chart' presents the flow chart of the proposed algorithm. The main conclusions of this work are presented in Section 'Conclusions'.

Principal component analysis

In high dimension problem, the feature extraction is transcendent, showing an understanding about signals and their different features. In this context, PCA is very useful and practical to make the database analysis, highlighting relevant information. PCA is appropriate to transform data from a high to low-dimension space, where scatter plots can be created. This transformation is done using eigenvalues and eigenvectors corresponding to the variance–covariance matrix, thus new signals called principal components (PCs) are calculated through a combination among original signals [46].

For example Fig. 1 shows original signals projected or transformed into this new axis, showing that signals can be better analyzed in a smaller dimension space.

PCA is used to analyze an offline original database, which can be reduced to another database of few dimensions, formed by new variables called principal components. Then, new signals can be online analyzed. Hence, their offline and online mathematical procedure is presented as follows.

Offline analysis

Eigenvalues and eigenvectors are PCA crucial features, which are usually obtained through the variance–covariance matrix **R**.

Let $x(n_1), x(n_2), x(n_3), \ldots, x(n_m)$ are the input signals, defined as:

$$\begin{aligned} x(n_1) &= [x_{1,1} \quad x_{1,2} \quad x_{1,3} \quad \ldots \quad x_{1,p}] \ \textit{first signal} \\ x(n_2) &= [x_{2,1} \quad x_{2,2} \quad x_{2,3} \quad \ldots \quad x_{2,p}] \ \textit{second signal} \\ x(n_m) &= [x_{m,1} \quad x_{m,2} \quad x_{m,3} \quad \ldots \quad x_{m,p}] \ m \ \textit{signal} \end{aligned} \tag{1}$$

Then, the data matrix denoted by **X** is:

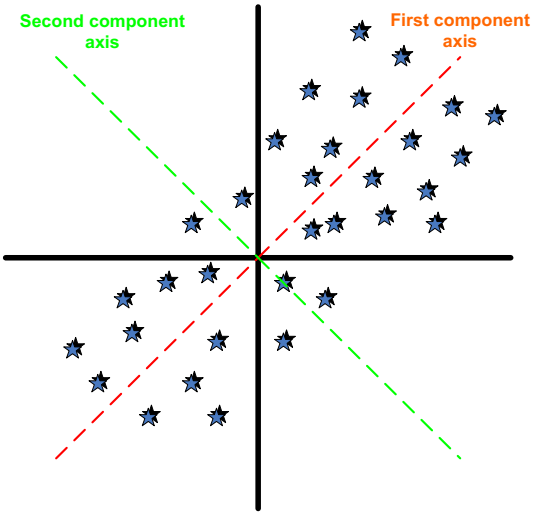

Fig. 1. Principal component sub-spaces.

$$X = \begin{bmatrix} x(1,1) & . & . & x(1,p) \\ x(2,1) & & & x(2,p) \\ . & & & . \\ x(m,1) & . & . & x(m,p) \end{bmatrix} \tag{2}$$

where m represents the signals number, p is the variables number. On the other hand, this matrix is usually normalized in order to get a maximum value 1. Later on, from this new matrix **Q**, their mean vector denoted by $\overline{Q}$ is extracted. Thus, their variance–covariance matrix **R** is calculated as follows:

$$R = \frac{\sum_{i=1}^{m}(Q_i - \overline{Q})(Q_i - \overline{Q})}{(m-1)} \tag{3}$$

where m represents the signals number, **Q** is the normalized data matrix under study and $\overline{Q}$ corresponds to their mean vector. Later on, from this matrix **R**, their eigenvalues and eigenvectors denoted by υ and ɣ are calculated, where:

$$\begin{aligned} \gamma(n_1) &= [\gamma_{1,1} \quad \gamma_{1,2} \quad \gamma_{1,3} \quad \cdots \quad \gamma_{1,p}]^T \ \textit{first eigenvector} \\ \gamma(n_2) &= [\gamma_{2,1} \quad \gamma_{2,2} \quad \gamma_{2,3} \quad \cdots \quad \gamma_{2,p}]^T \ \textit{second eigenvector} \\ \gamma(n_p) &= [\gamma_{m,1} \quad \gamma_{m,2} \quad \gamma_{m,3} \quad \cdots \quad \gamma_{p,p}]^T \ p \ \textit{eigenvector} \end{aligned} \tag{4}$$

$$\upsilon = [\upsilon_1 \quad \upsilon_2 \quad \upsilon_3 \quad \ldots \quad \upsilon_p] \ \textit{eigenvalues} \tag{5}$$

where p represents the number of variables, T represents transposed. It is necessary to note that there are p eigenvectors and p eigenvalues. Finally, by using these eigenvectors, principal components $y(n_m)$ are calculated as:

$$\begin{aligned} y(n_1) &= [q_{1,1} \quad q_{1,2} \quad q_{1,3} \quad \cdots \quad q_{1,p}] * [\gamma_{1,1} \quad \gamma_{1,2} \quad \gamma_{1,3} \quad \cdots \quad \gamma_{1,p}]^T \\ y(n_2) &= [q_{2,1} \quad q_{2,2} \quad q_{2,3} \quad \cdots \quad q_{2,p}] * [\gamma_{2,1} \quad \gamma_{2,2} \quad \gamma_{2,3} \quad \cdots \quad \gamma_{2,p}]^T \\ y(n_m) &= [q_{m,1} \quad q_{m,2} \quad q_{m,3} \quad \cdots \quad q_{m,p}] * [\gamma_{1,1} \quad \gamma_{1,2} \quad \gamma_{1,3} \quad \cdots \quad \gamma_{1,p}]^T \end{aligned} \tag{6}$$

where $y(n_1)$ represents the first principal component. Their matrix **Y** is represented by:

$$[Y] = [Q][\gamma] \tag{7}$$

where **Q** is the normalized data matrix, and ɣ represents the eigenvectors matrix, respectively.

Online analysis

PCA has an important characteristic, which is that after that the data matrix is offline analyzed, their eigenvectors are extracted. In this context, a new signal can be online analyzed by using only these eigenvectors. Thus, real-time signals can be continuously analyzed in Electric Power Systems. A new signal is analyzed as follows:

Let $w(n_1)$ is the new signal defined as:

$$w(n_1) = [w_{1,1} \quad w_{1,2} \quad w_{1,3} \quad \dots \quad w_{1,p}] \tag{8}$$

Later on, the principal components of this new signal are calculated like:

$$y(w) = \left(w(n) - \overline{Q}\right) * \gamma(n) \tag{9}$$

where γ represents the eigenvectors, $\overline{Q}$ is the mean vector of the **X** normalized database. Based on the previous said, it is possible to see that only apply Eq. (9), a new signal can be online analyzed.

Eigenvalues and eigenvectors

Eigenvalues and eigenvectors are used to obtain principal components, which make an eigen-decomposition of the matrix **R**. Accordingly, by using those features, an intrinsic structure of the matrix can be extracted. The eigenvectors may be optimally extracted and selected based on their variance, which is a great characteristic of PCA. For example, wavelet analysis and mathematical morphology widely used to develop EPS algorithms use a function called mother wavelet and a structuring element, respectively. However, there are not specific guidelines for the selection of these functions. Therefore, a very important feature of PCA is how extract eigenvectors optimally. The eigenvector depend on the length of the signal, i.e. the number of variables under study.

Electric power system

The 220 kV power system illustrated in Fig. 2 is used to study the detection-identification algorithm. The EPS is simulated through the ATP/EMTP software [47], where different switching operation and lightning stroke conditions were simulated. This work uses voltage travelling waves recorded by relay R1 at bus M with a 1 MHz sample frequency. The EPS contains 6 buses, 5 single transmission lines, 2 transformers and 6 generators. In this EPS, the 220 kV transmission lines denoted as M–N and two-ground wires were modelled with the frequency dependent model. Besides that, extensive simulation studies are carried out for different combinations of flash peak current magnitude, positive and negative polarity, tower footing resistance (TFR), lightning stroke on the tower, on phase directly or on mid-span. Furthermore, different switching operations with different inception angle, loads and others are running. On the other hand, in order to consider the variation of parameters considering the frequency, the transmission line is simulated using the frequency-dependent parameter line model. By using this model, a more accurate representation of a wide range of frequencies contained in transient phenomena can be simulated. Besides that, in this paper, the signals used were simulated, real signals were not used because currently there are not ones recovered for any protection relay at 1 MHz sample frequency.

Switching operation and lightning stroke signals simulated

Lightning stroke is considered as a current source. Measurements of lightning strokes have shown that those signals are negative and positive polarity with quite variable flash peak current amplitude (FPCA) [1,48,49]; it may be as low as a few thousand amperes (5 kA) and as high as several hundred thousand amperes (200 kA). Thus, this variation is imperative in lightning studies on TLs. As proposed by [48], by using the Heidler model in the ATP/EMTP software, the flash current can be represented. In this context, different positive and negative lightning stroke signals with value ranges of FPCA = 6–6, 2–8 ... 250 kA along the transmission line M–N are considered.

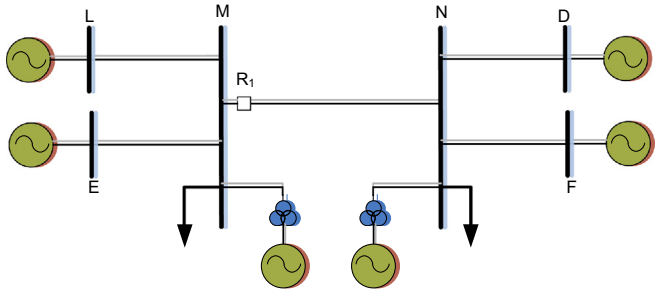

Fig. 2. Power system.

On the other hand, based on reports presented by different organizations, correct simulations of switching operations can be developed [50–53]. Several EPS maneuvers can produce switching overvoltages. However, these reports indicate that the main overvoltages are produced by line energization and des-energization. In this context, in this research, the authors have considered those switching operations and also switching of loads and transformers.

Regarding to the inception angle of switching or lightning stroke (disturbance start), these signals were simulated considering different inception angle. Therefore, transient signals corresponding to switching operations and lightning strokes were run with different inception angles from 0° to 360°, respectively. Table 1 presents a summary of different scenarios simulated in this paper.

Besides that, in the ATP software, the step size Δt must be adequately selected in order that the EPS model run. In this context, there are two forms to select Δt. First: Δt can be chosen based on the maximum frequency, so the Nyquist theorem must be used. Second: Δt can be chosen based on the shortest line. Thus, the step size Δt must be less than the travel time of the shortest line on the network. In this proposed paper, Δt is chosen based on the shortest line on the network, which is simulated using distributed. Based on the above said, in this paper considering this length, a step size Δt of 1 μs is adequate. It is necessary to note that independently of the frequency of simulated signals, if the step size Δt is not chosen based on the shortest line section, the model developed in ATP does not run, it is because the shortest line section must be simulated by distributed parameter models.

Proposed methodology

The proposed methodology has two operating stages; the first is related to the phenomena detection. While, the second is used to make the phenomena identification. In this work, switching operations or lightning strokes are considered. In the following the proposed methodology is presented.

Detection algorithm

Protection schemes must detect fault signals as quickly as possible; initiating or not correction actions. Hence, by processing registered signals, the first wave-front can be detected. Therefore, by

Table 1
Summary of different scenarios of lightning strokes and switching operations simulated.

	Lightning feautres					Point of impact				Distance from R1 at M bus
	Ip (kA)	Polarity		TFR	Inception angle	On tower	On phase wire directly	Impacted phase	On mid-span shiel wire	On mid-span phase wire	Voltage waves corresponding to different lightning stroke distances from 1 km to the total distance with 1 km step were run
		Positive	Negative								
Lightning strokes	6, 6.2, 7, 7.5,	√	√	10	0	√	√	R,T	√	√	
	8.5, 9, 9.5, 10,	√	√	20	45	√	√	R,T	√	√	
	20, 80, 100,	√	√	30	90	√	√	R,T	√	√	
	111, 120, 143,	√	√	50	120	√	√	R,T	√	√	
	160, 170, 200, 220,250kA	√	√	200	270	√	√	R,T	√	√	

Ip: Flash peak current amplitude
TFR: Tower footing resistance

Switching operations	Switching phase			Switching instants
	R	S	T	
Line energization	√	√	√	$T = t1 - T = t17$,
Line desenergization	√	√	√	0°, 20°, 40°, 60°,
Load switching on	√	√	√	80° …, 340°
Load switching off	√	√	√	
Transformer switching	√	√	√	

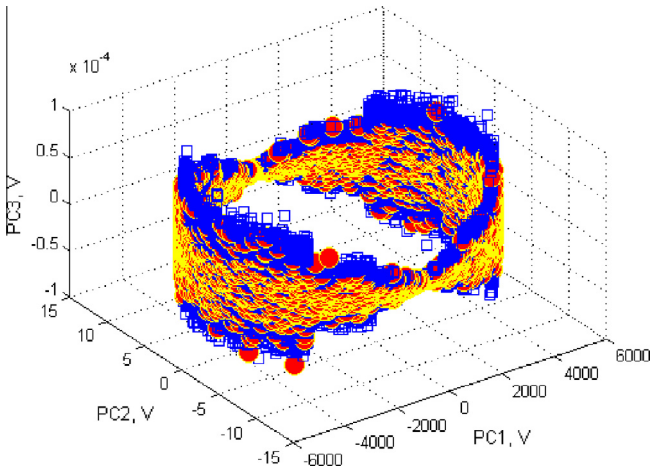

Fig. 3. Ellipsoidal pattern corresponding to three phase voltage signals during normal operating conditions.

taking as base the transmission line operation voltage x, an Ellipsoidal Pattern (EP) that represents their operational state can be determined. Thus, when any disturbance is generated, their first wave-front of incremental signals Δx_1 is generated, which has a different characteristic to that corresponding to the EP.

Application of PCA to normal operation condition

Voltage signals for this stage are $f(x)$ discrete sinusoidal waves registered in one-cycle data window. Notwithstanding, in order to disclose the variation of these signals and to obtain features patterns, those signals are decomposed and analyzed at different data windows of 25 samples with 1 μs between samples.

Thus, each data window has 25 points with 1 μs step, i.e. the voltage signals in normal operation are represented like p-dimensional vectors such as:

$$x_j = [x_{1,1} \quad x_{1,2} \quad x_{1,3} \quad x_{1,4} \quad \dots \quad x_{1,p}] \tag{10}$$

where p represents the voltage signals value in normal operation. Therefore, a total of 2400 voltage signals represented like 1×25 row vectors are used to form the matrix **X** as follows:

$$X = \begin{bmatrix} x(1,1) & . & . & x(1,p) \\ x(2,1) & & & x(2,p) \\ . & & & . \\ x(n,1) & . & . & x(n,p) \end{bmatrix} \tag{11}$$

where n and p represent the number of observations and variables, respectively. The next mathematical process is applied to their standardized matrix **J,** thus, supposing that $j_1, j_2, \dots, j_p$ are 1×25 row vectors, the steps to calculate PCs in normal state are:

- To subtract the mean vector of size (1×25)

$$\bar{j} = \left[\frac{\sum_{i=1}^{n} j(i,1)}{n} \quad \frac{\sum_{i=1}^{n} j(i,2)}{n} \quad \frac{\sum_{i=1}^{n} j(i,3)}{n} \quad \frac{\sum_{i=1}^{n} j(i,4)}{n} \quad \dots \quad \frac{\sum_{i=1}^{n} j(i,p)}{n} \right] \tag{12}$$

- To calculate the variance–covariance matrix, $S = 25 \times 25$

$$S = \frac{\sum_{i=1}^{n} (j_i - \bar{j})(j_i - \bar{j})}{(n-1)} \tag{13}$$

- To compute eigenvalues of matrix S, 25 eigenvalues

$$\lambda_1 > \lambda_2 > \lambda_3 \dots > \lambda_{25} \tag{14}$$

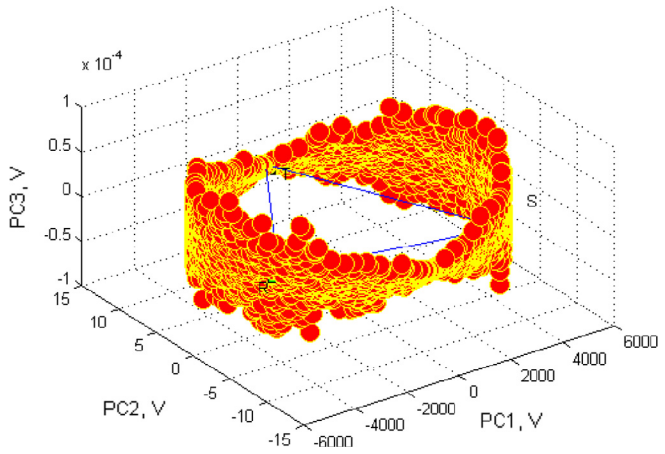

(a) Three dimensions in PCA subspace.

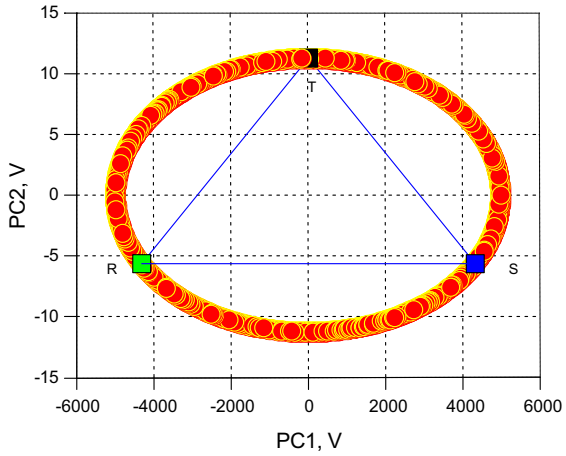

(b) Two dimensions in PCA subspace.

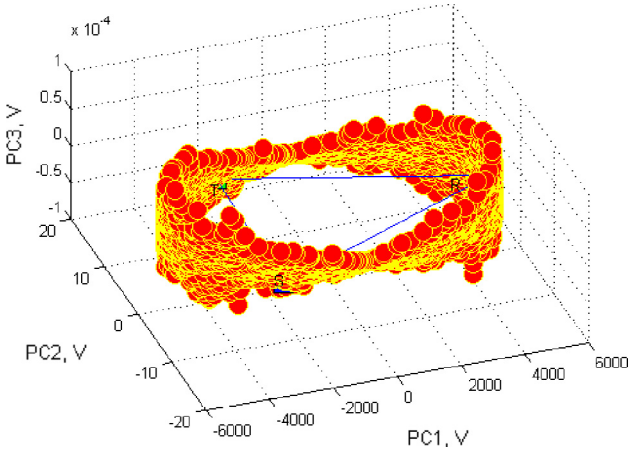

(c) Three dimensions in PCA subspace.

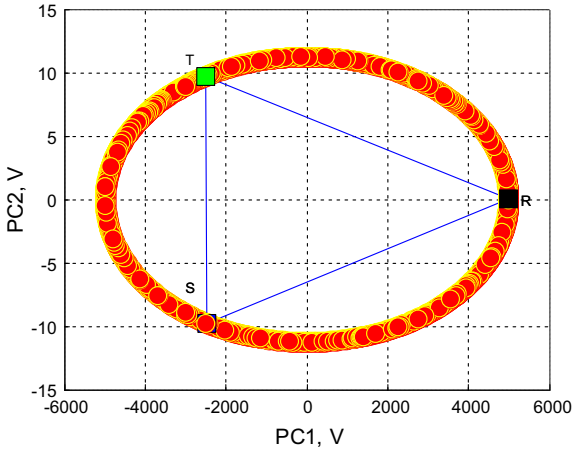

(d) Two dimensions in PCA subspace.

Fig. 4. Three phase voltage signal during normal operating conditions (a and c) three dimensions in PCA subspace; (b and d) two dimensions in PCA subspace.

- To compute eigenvectors of matrix S, 25 eigenvectors

$$\mu_1, \mu_2, \mu_3, \ldots, \mu_{25} \tag{15}$$

- To compute the Principal Components, (2400 × 25)

$$\begin{bmatrix} z_1 \\ z_2 \\ \ldots \\ z_n \end{bmatrix} = \begin{bmatrix} \mu_1^T \\ \mu_2^T \\ \ldots \\ \mu_n^T \end{bmatrix} (j - \bar{j}) = U^T (j - \bar{j}) \tag{16}$$

Geometrical interpretation and pattern extraction in normal operation

After being processed normal operation signals through PCA, those signals are sequentially projected on the PC coordinates, i.e. the first data window of 25 points is projected on the PC coordinates, later on, a new sample becomes available, the oldest samples value is discarded and the new sample values are projected. Then, each sample is used for calculations, successively. This process is made to complete a voltage signal cycle. By projecting those normal operation signals on the PC coordinates, it is possible to determine that those signals describe an Ellipsoidal Pattern (EP) very well detailed. Figs. 3 and 4 illustrates those signals projected at 2 and 3-dimensions PC sub-space.

From Figs. 3 and 4 it is possible to see that the Ellipsoidal Pattern (EP) describes completely the normal state of the transmission line. Accordingly, based on the EP and their PCs values calculated (see Table 1); it is possible to establish the transmission line performance as follows:

First: It is well known that in normal operation, the overall sum of voltage signals is zero. Thus, by using PCA a similar condition is also achieved. I.e. those signals projected on the Ellipsoidal Pattern always form a triangle–rectangle; the overall sum of the first two PCs (in this paper is called STC) of the three phases is always a fixed absolute value ε_0. For instance, in Fig. 4a and b the red line[1] Ellipsoidal Patterns indicate the normal operating conditions and the blue line trajectories placed inside the ellipsoidal pattern indicate the triangle–rectangle formed by the first two PCs of each phase. Thus, the overall sum of the three phases R, S and T in the sub-space of the principal components is always that value ε_0. STC can be calculated such as:

$$\mathrm{STC} = \sum_{i=1}^{r} (\mathrm{PC}_{1i} + \mathrm{PC}_{2i}) \tag{17}$$

[1] For interpretation of color in Figs. 4, 9 and 10, the reader is referred to the web version of this article.

Table 2
Calculated values of STC, TPC and EE during normal operating conditions.

Transmission line phases	Principal components							STC	EE
	PC_1	PC_2	PC_3	PC_4	PC_5	PC_9	PC_{10}		
Phase R	2378.71	9.84	0	0	0	0	0	30.86	0.99
Phase S	−4998.75	−0.25	0	0	0	0	0		1
Phase T	2589.23	−9.65	0	0	0	0	0		1
Phase R	2380.07	9.84	0	0	0	0	0	30.86	0.99
Phase S	−4998.78	−0.24	0	0	0	0	0		1
Phase T	2587.89	−9.65	0	0	0	0	0		1
Phase R	2381.44	9.84	0	0	0	0	0	30.86	0.99
Phase S	−4998.82	−0.24	0	0	0	0	0		1
Phase T	2586.55	−9.65	0	0	0	0	0		1

PC: number of principal component.
STC: Overall sumatory of first two principal components of three phases.
EE: Calculated value based on the equation of the ellipse.

where PC_1 and PC_2 are the first two PCs and r is the phase selected (phase R, S, T). The magnitudes of some STC are given in Table 2. Concluding, by using Eq. (17), the STC values can be determined and the normal operation condition can be verified.

Second: From Fig. 4a and c, it is possible to verify that the third PC value and other PCs different to the first two PCs are close to zero, i.e. the magnitude from the third PC to the twenty-five PC (in this paper is called TPC) will be always zero except when it involves the first two PCs.

For example, in Table 2 it is summarized those results from the third PC to the tenth PC for TPC. Therefore, calculating the TPC value from any PCs, normal operation condition can be determined as follows:

$$\mathrm{TPC} = \begin{bmatrix} \mu_3^T \\ \mu_4^T \\ \cdots \\ \mu_{25}^T \end{bmatrix} (j - \bar{j}) \tag{18}$$

where μ are eigenvectors different to $\mu 1$ and $\mu 2$.

Third: By projecting waveforms on the PCs coordinates, it was found that those signals describe perfectly an Ellipsoidal Pattern (EP). See Fig. 4b and d. From these figures, it is clear that the graph is symmetric with respect to the PC_1 axis, PC_2 axis, and the origin. Hence, using the definition and equation of the ellipse [54], an equation for an ellipse located in the PCs coordinate system is determined.

The standard equation of an ellipse with center at (0,0) is given by:

$$\frac{x^2}{a^2} + \frac{y^2}{b^2} = 1 \quad a > b > 0 \tag{19}$$

where the curve is described by two lengths, a and b. The longer axis a, is called the semi-major axis. On the other hand, the shorter axis b is called the semi-minor axis [54].

Therefore, in order to adapt the Ellipsoidal Pattern data to the standard equation of the ellipse, Eq. (19), it is necessary to extract values of a and b, which in the PC subspace are represented by $PC_{1\max}$ and $PC_{2\max}$ respectively, shown in Fig. 5. Those values corresponding to $PC_{1\max}$ and $PC_{2\max}$ are 5000 and 11.2819, respectively.

After, replacing those values in the standard form, an equation that represents the normal operation condition is determined such as:

$$\mathrm{EE} = \frac{PC_{1r}^2}{PC_{1\,\max}^2} + \frac{PC_{2r}^2}{PC_{2\,\max}^2} \approx 1 \tag{20}$$

where PC_{1r} and PC_{2r} are the first two PCs of any phase r and EE in this paper represents the calculated value based on the equation of the ellipse. The evaluation of EE with some PCs in the normal state is given in Table 2.

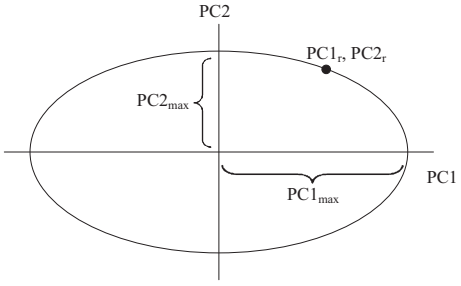

Fig. 5. Ellipsoidal pattern in the PCA subspace.

Disturbance detection criteria

By using STC, TPC or EE, three different conditions for phenomena detection are formulated. Therefore, as long as the transmission line works normally, STC = ε_0 = 30.86, TPC = 0, and EE = 1 are obtained. However, if those values are different, a disturbance is detected. Detection criteria are shown in Table 3.

Identification algorithm

After detecting the phenomenon, the stage two starts working, where it calculates Euclidean Norm (EN) for each of the following 50 consecutive samples coming. At the end of the 50 samples, EN values are summed to find a threshold value (ε) useful for the switching operations identification.

Projection of signals on ellipsoidal pattern

The discrete time signal $f(x)$ of 25 points (1 × 25 row vector) is projected onto a new base. Hence, since the reference database corresponding to the Ellipsoidal Pattern is in PCs, it is necessary that the new row vector is projected in the Ellipsoidal Pattern coordinates. Therefore, this projection must be made using those coefficients given by the eigenvector of the variance–covariance matrix of the original data as:

$$f(pc) = \left(f(x) - \bar{j}\right) \times U \tag{21}$$

where **U** is the matrix of PC coefficients, $\bar{j}$ is the 1 × 25 mean vector of the Ellipsoidal Pattern and $f(pc)$ is the new row vector. Therefore, using those eigenvectors, test signals are projected in the 2-dimension and 3-dimension space of the previously Ellipsoidal Pattern established. For instance, Fig. 6 shows the disturbance projected on the PCs plane with 9 new vectors, while, Fig. 7 shows 70

Table 3
Detection criteria for disturbance detection.

Normal operation condition					Disturbance detection condition				
STC = 30.86	or	TPC = 0	or	EE = 1	STC ≠ 30.86	or	TPC ≠ 0	or	EE ≠ 1

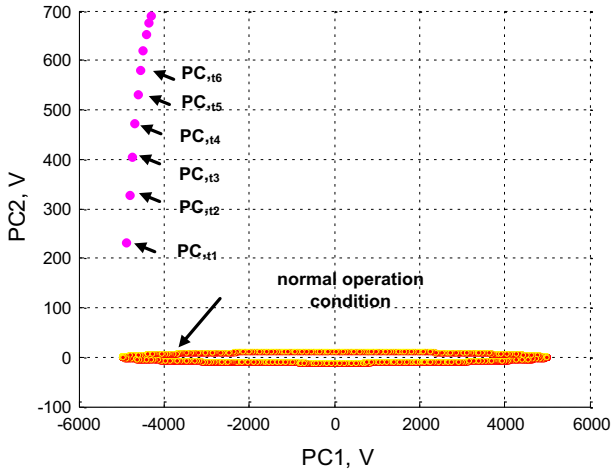

Fig. 6. Disturbance projected on ellipsoidal pattern coordinates.

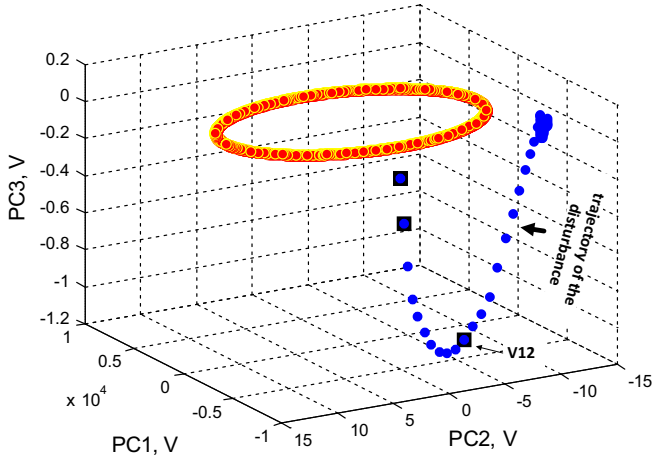

Fig. 7. Switching projected on ellipsoidal pattern coordinates.

new vectors of a switching operation projected on the Ellipsoidal Pattern, i.e. the new data window of 25 points is projected on the PC coordinates, later on, a new sample becomes available, the oldest of the samples value is discarded and the new data window is projected on the PC coordinates.

Trajectories extraction

From Figs. 6 and 7 it can be seen that PCs values present patterns, indicating the trajectory of the disturbance type. Based on this characteristic, and finding the overall sum of the Euclidean Norm (EN) between PCs for each new sample and the reference ellipsoidal surface, the type of phenomena can be identified.

On the other hand, Fig. 8 shows Euclidean distances (d) of the first eight new vectors, which are calculated as follows:

$$d(f,f_o) = \Delta dk = \sqrt{\sum_{i=1}^{h}(f_i - f_{oi})^2} \tag{22}$$

where f_o is the reference ellipsoidal pattern center (0,0) and h is the number of PCs chosen (h = 2, the second and third eigenvector).

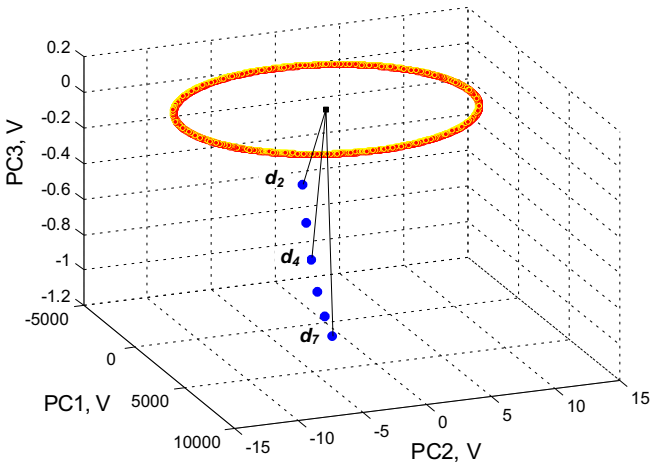

Fig. 8. Distance from ellipsoidal pattern center to PCs.

In this context, those PCs of each new vector can be obtained and from the Euclidean distance (Δdk) it is possible to determine a criterion to identify switching operations. Hence, Δdk, with k = 1, 2, 3, . . . , n, corresponds to the distance between PCs for each sample and the reference ellipsoidal surface (0,0). Later, in order to calculate the amount of energy contained in Δdk, the Euclidean Norm (EN) of Δdk is calculated by:

$$\mathrm{EN} = \sqrt{\sum_{k=1}^{n}\Delta d^2(k)} \tag{23}$$

where n is the number of samples selected after the disturbance is detected. Therefore, those discrimination components can be derived as follows:

$$F = \begin{cases} 1 & \mathrm{EN} > \varepsilon \\ 0 & \mathrm{EN} \leqslant \varepsilon \end{cases} \tag{24}$$

where ε is a threshold value that in this research is determined considering a counting scheme, and F is a logic value that is used as a discriminator element. Therefore, the disturbance type identification is performed by computing norms of n new consecutive vectors. Since the Euclidean norm values of switching operations are smaller than of lightning strokes, if the Euclidean Norm value is smaller than the threshold value, a switching operation is identified.

Continuous PCs calculation

This methodology assures that when a switching operation on the transmission line is produced, the relay will not trigger, which is based on a continuous PCs and Euclidean Norm calculation. In this context, continuous here means, for example, that for each 1 μs step, both the principal component value and the Euclidean Norm (EN) value are calculated and added to the EN calculation of the previous 1 μs. I.e. the next PC and EN that must be calculated 1 μs later, and are added to the previous EN. After 50 calculations, the total EN value is compared with the threshold value ε. If the EN value exceeds the threshold value ε, a condition different to a switching operation is detected. Therefore, in order to secure the identification of switching operations, a counting scheme is used. Initially the counter is set to zero and increase it by one when

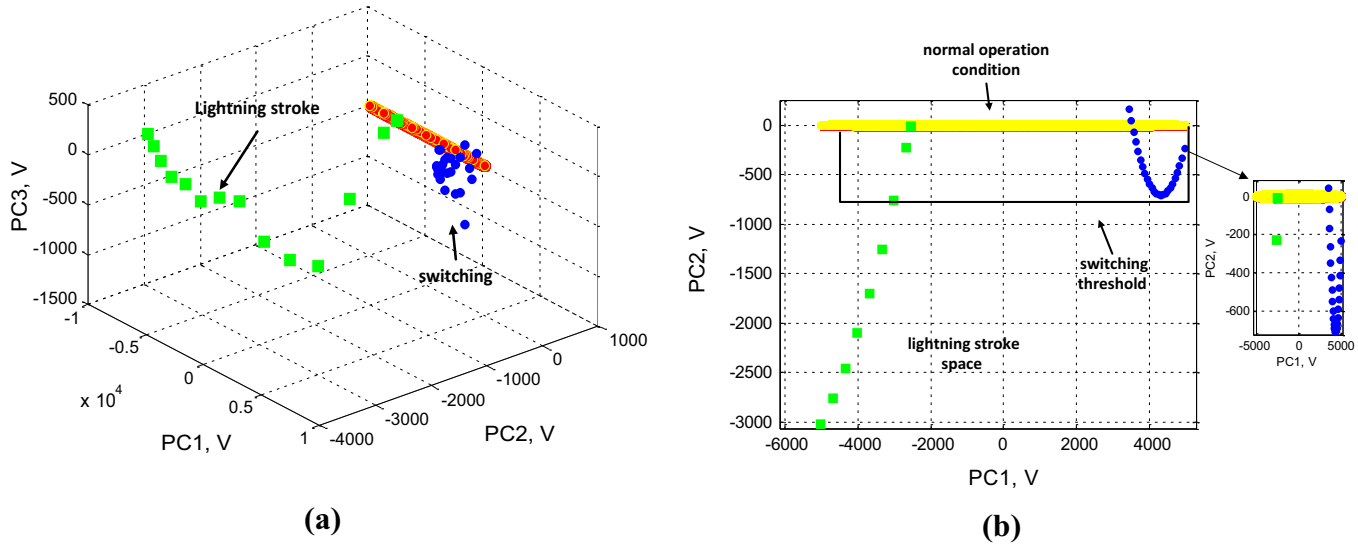

Fig. 9. Trajectory of lightning stroke and switching operations (a) 3D; (b) 2D.

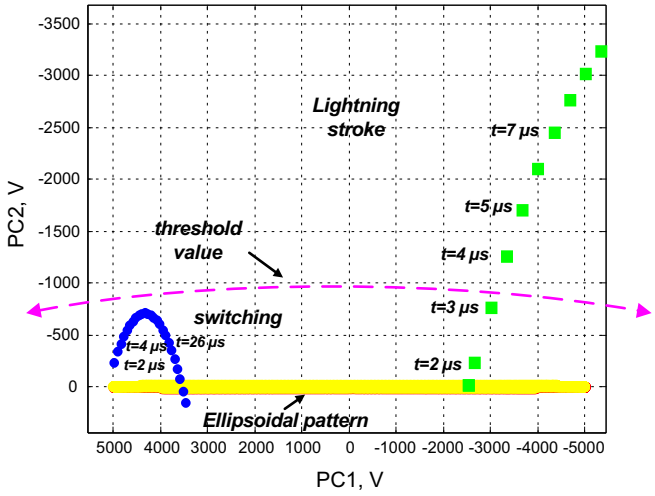

Fig. 10. Actuation zones for switching operations and lightning stroke.

the disturbance has been detected. In this work a count of 50 is used.

Selection of a threshold value

As regards to the threshold value, by using PCA is possible to determine that switching operations define an actuation zone. Figs. 9 and 10 shows the trajectories for switching operations and lightning strokes. Hence, a Euclidean Norm threshold value is determined as $\varepsilon < 6000$. It is very important to note that the switching operations Euclidean Norm value is smaller than the border value.

From Figs. 9 and 10, the red line ellipsoidal pattern indicates the normal operating condition, the pattern with blue line trajectory placed outside the ellipsoidal pattern indicates the line switching, and finally the trajectory displayed with green line indicates a lightning stroke.

Moreover, from previous figures it is possible to see that when a switching occurs, their trajectory moves slowly from the ellipsoidal pattern to the location generated by switching operations. On the other hand, during a lightning stroke, the trajectory of the second and third principal component quickly moves on the PCs plane.

Performance evaluation

Evaluation of the detection algorithm

In this paper, two algorithms corresponding to the transient signal detection and switching operations and lightning strokes identification, are presented. It is imperative to note that the detection algorithm shown in Figs. 3 and 4, only represents how the transmission line performance in normal operation conditions by using STC, TPC or EE, is represented. On the other hand, after that a transient signal produced by different phenomena (in this paper is produced by switching operations or lightning strokes), is detected, then the second algorithm starts running. The second algorithm function is to make the identification that phenomena is produced, either switching operation or lightning stroke. In this context, in this paper the second algorithm is presented from Figs. 6–10, where the EN term is used.

Based on the above said, it is clear that in Fig. 11, the detection algorithm evaluation, is only presented. Regarding to the identification algorithm evaluation between switching operations and lightning strokes, it is presented in Section 'Identification algorithm evaluation during switching operations'.

Regarding to the detection algorithm, their performance was tested by using different simulated signals of either switching operations or lightning strokes. Accordingly, those signals obtained after simulations are computed and projected in the multidimensional space corresponding to the Ellipsoidal Pattern. Fig. 11a–d presents some transient signals projected on the Ellipsoidal Pattern.

In normal operation condition (i.e. when a transient signal is not present), it can be determined that their signals are represented by an Ellipsoidal Pattern, where STC is a constant absolute value, and TPC is approximately zero. See Figs. 3 and 4, respectively. However, From Fig. 11, it is possible to see that during disturbance presence, their behavior is different. Hence, not only those values of STC, TPC and EE change rapidly, but also their trajectories are located outside of the Ellipsoidal Pattern. For example, in Fig. 11 and Table 4, it is clear that the STC, TPC and EE values are different to those values presented in Table 2. Therefore, the TPC values in Table 4 represented by PC_3, PC_4, PC_5 to PC_{25} are different to zero. Hence, based on Table 3, a transient signal is detected.

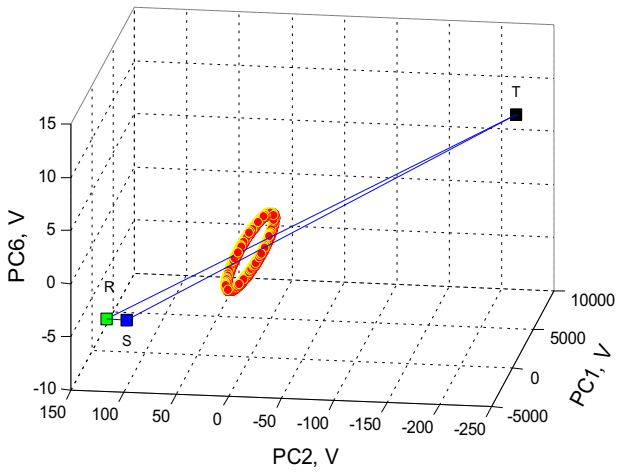

(a) Projection of PCs during first signal.

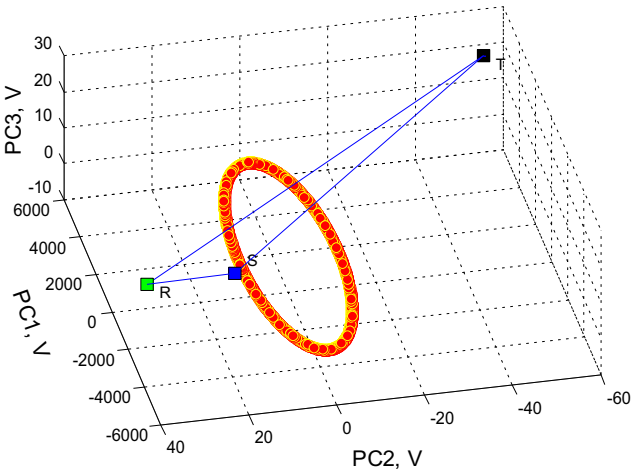

(b) Projection of PCs during second signal.

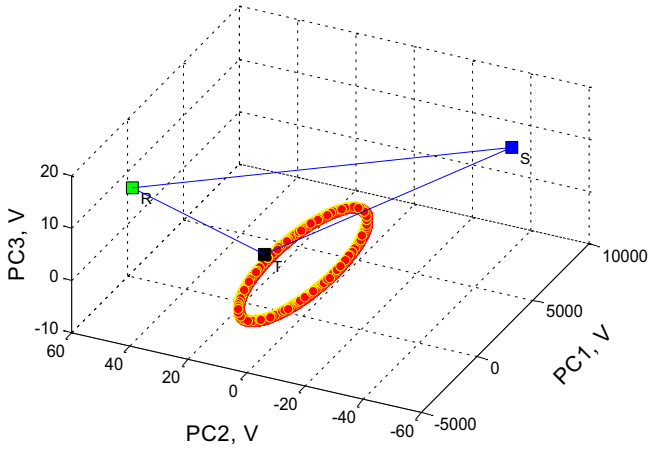

(c) Projection of PCs during third signal.

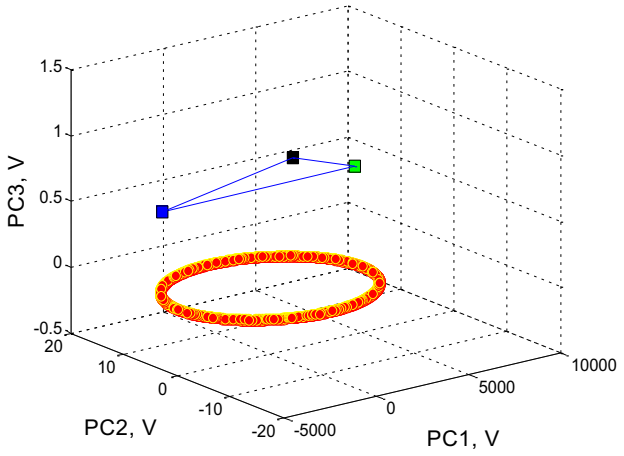

(d) Projection of PCs during fourth signal.

Fig. 11. (a) Projection of PCs during first signal. (b) Projection of PCs during second signal. (c) Projection of PCs during third signal. (d) Projection of PCs during fourth signal.

Table 4
Calculated values of STC, TPC and EE.

Figure	Transmission line phases	Principal components						STC	EE
		PC_1	PC_2	PC_3	PC_4	PC_6	PC_{10}		
Fig. 11a	Phase R	−2492.02	126.21	46.48	21.94	5.09	16.72	0.15	125.4
	Phase S	−2486.9	107.45	47.01	22.19	−5.14	−16.91		90.96
	Phase T	4979.08	−233.66	93.49	−44.14	10.23	33.63		429.96
Fig. 11b	Phase R	−2566.64	36.9	10.72	5.06	−1.17	−3.86	0.15	10.96
	Phase S	−2554.78	16.91	10.81	5.1	−1.18	−3.89		2.51
	Phase T	5121.56	−53.81	21.53	−10.17	2.36	7.75		23.8
Fig. 11c	Phase R	−4512.74	41.34	19.02	8.98	−2.08	−6.84	0.15	14.24
	Phase S	4609.42	−54.15	19.34	−9.13	2.12	6.96		23.89
	Phase T	−96.53	12.81	0.32	0.15	−0.04	−0.12		1.29
Fig. 11d	Phase R	5121.39	1.85	0.73	0.34	−0.08	−0.26	0.15	1.08
	Phase S	−2573.99	11.24	0.49	0.23	−0.05	−0.17		1.26
	Phase T	−2547.36	−13.29	1.29	−0.61	0.14	0.46		1.65

PC: number of principal component.
STC: Overall sumatory of first two principal components of three phases.
EE: Calculated value based on the equation of the ellipse.

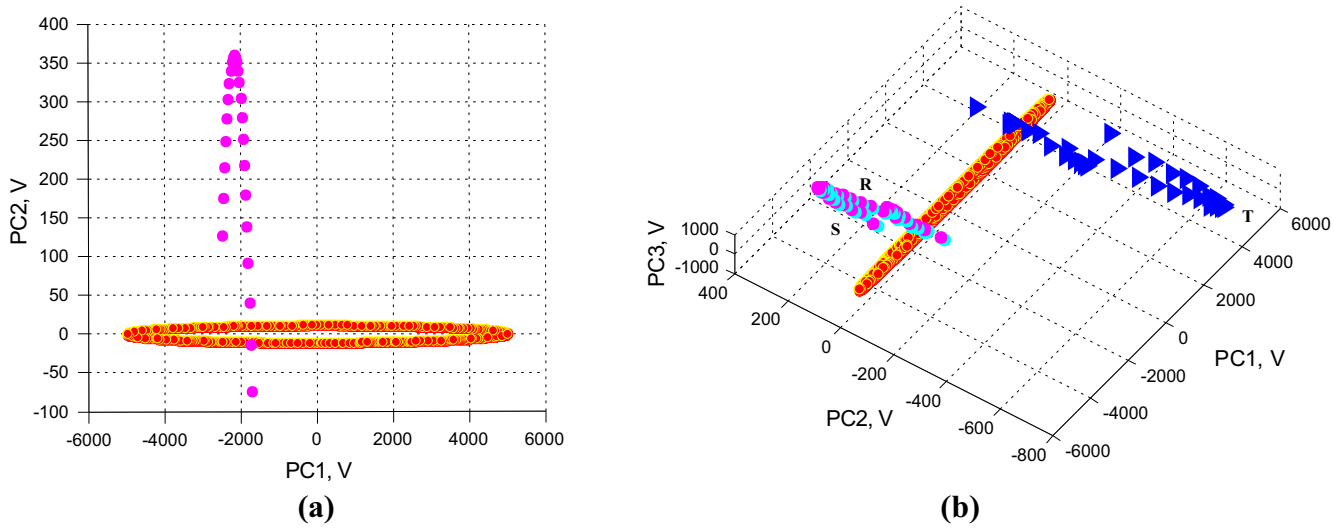

Fig. 12. Behavior of the PCs during a line energization. (a) Phase R; (b) three phases.

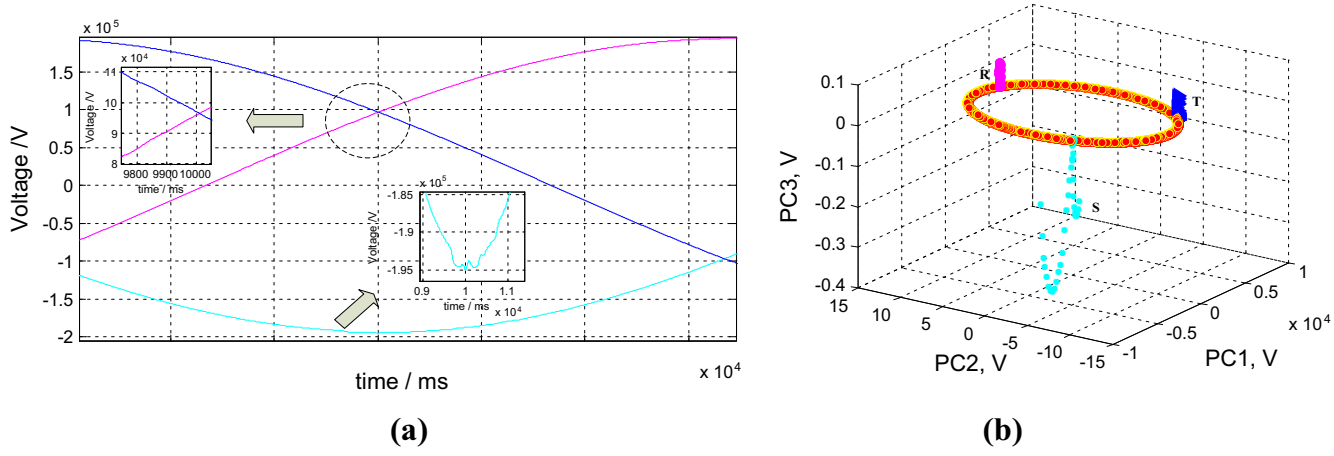

Fig. 13. Behavior of the PCs during a line desenergization. (a) Three phase voltage signals; (b) three phases PCs.

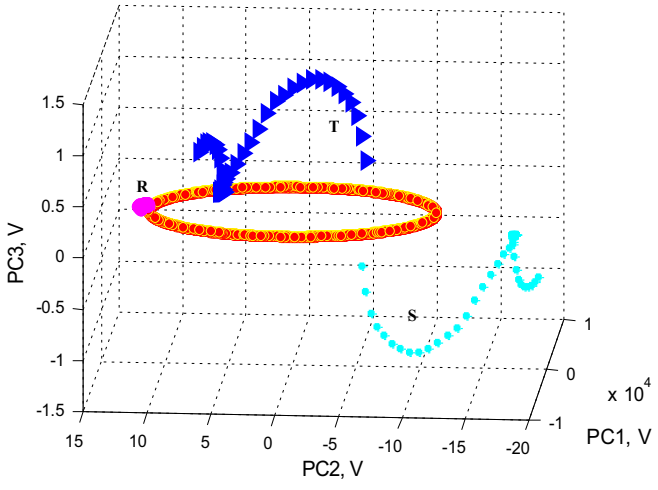

Fig. 14. Behavior of the PCs during transformer switching.

Table 5
EN values for some testing switching operations.

Figure	Switching	EN		
		Phase R	Phase S	Phase T
Fig. 12	Line energization from bus M to bus N en t = t1	1728	1669	3396
	Line energization from bus M to bus N en t = t2	2248	3328	1082
	Line energization from bus M to bus L	1679	1615	3294
Fig. 13	line desenergization from bus M to bus L	73	34	64
	Line energization from bus M to bus E	4512	4545	108
	Line desenergization from bus M to bus E	64	76	78
	Load switching on at bus M	105	39	77
	Load switching off at bus M	105	11	55
Fig. 14	Transformer switching at bus M	80	114	41

Identification algorithm evaluation during switching operations

In order to verify the performance of the identification algorithm, different signals of switching operations are tested. Thus, after the disturbance has been detected, the switching overvoltage can be computed as in Eq. (21). According to Figs. 9 and 10, when the switching occurs, their PCs instantaneously change from the Ellipsoidal Pattern to another pattern with a different trajectory outside of the EP characteristic zone. Those three phase voltages

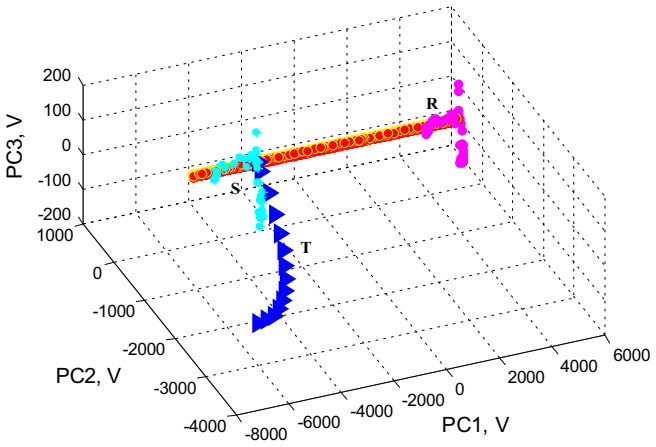

Fig. 15. Trajectories during lightning stroke # 1.

and trajectories during different switching operations like switching on, switching off and others are shown from Figs. 12–14.

On the other hand, Table 5 shows those Euclidean Norm values during different switching operations. In this Table, it is possible to see that the EN value is still below the threshold value. These results show that the relay identifies correctly switching operations.

Identification algorithm evaluation during lightning stroke

From Figs. 9 and 10 it is also possible to see that during lightning strokes, their Euclidean Norm values will change rapidly exceeding the threshold value ε. Those three phases overvoltages and their trajectories during different lightning stroke types, magnitude, stroke on live wire, stroke on transmission tower and others are shown from Figs. 15 and 16. Furthermore, Table 6 shows their EN values.

Besides that, based on results it is necessary to note that independently of the inception angle used, not only the detection algorithm, but also the deterministic algorithm proposed in this paper correctly to make the identification of switching operations.

Additionally, as regards to the useful information of each data window, these algorithms were tested with transient signals whose data window range varies from 25 μs to 50 μs. However, after that a lot of simulated signals were tested, it is possible to determine that a minimum data window of 25 μs gives acceptable results.

On the other hand, regarding to the data window size, it is well known that traditional protection algorithms use data window of 1 cycle, 16–20 ms approximately. However, in order to develop an ultra-high speed deterministic algorithm, it is necessary to consider two issues as follows.

The protection algorithm operation time is determined by the data window size and by the time data processing, which currently due to the technological advance, this time is very short. In this context, in order to assess the response performance of these proposed algorithms. They use data windows of 25 μs composed by transient signals produced by either switching operations or lightning strokes, which are sampled to a sampling rate of 1 MHz, i.e. each point is discretized to 1 μs. Therefore, the data window used in this paper is smaller than that data window used by traditional protection relays.

On the other hand, regarding to the time data processing, by using the operations number (225 for the detection algorithm and 150 for the identification algorithm), and the relaying microcontroller processing time (1 ns for each operation) [55,56], the top time is 0.225 μs and 0.15 μs, respectively. These times are smaller than the time step along samples.

Based on the above said, it is clear that not only the data window size used in this paper, but also the microcontroller processing time are short. Therefore, the protection algorithm total time is very small, which can be considered of ultra-high speed.

Flow chart

In Fig. 17 the detection and identification algorithm flow chart is presented. It assures that due to switching operations the protection relay does not trigger. Accordingly, if the EN value does not exceed the threshold value, a switching operation is identified. However, if the EN value exceeds the threshold value, a lightning stroke is identified.

The PCs quantities marked with the subscript set of samples are assigned the Euclidean Norm fixed value by the protection relay. Hence, the remaining quantities are continuously updated by the relay during the disturbance. Where, the switching operation identification is carried out by comparing the fixed Euclidean Norm value ε with the value continuously updated (50 μs). Finally, when the updated EN value exceeds the fixed value ε, a lightning stroke on transmission line is detected. Therefore, by studying the

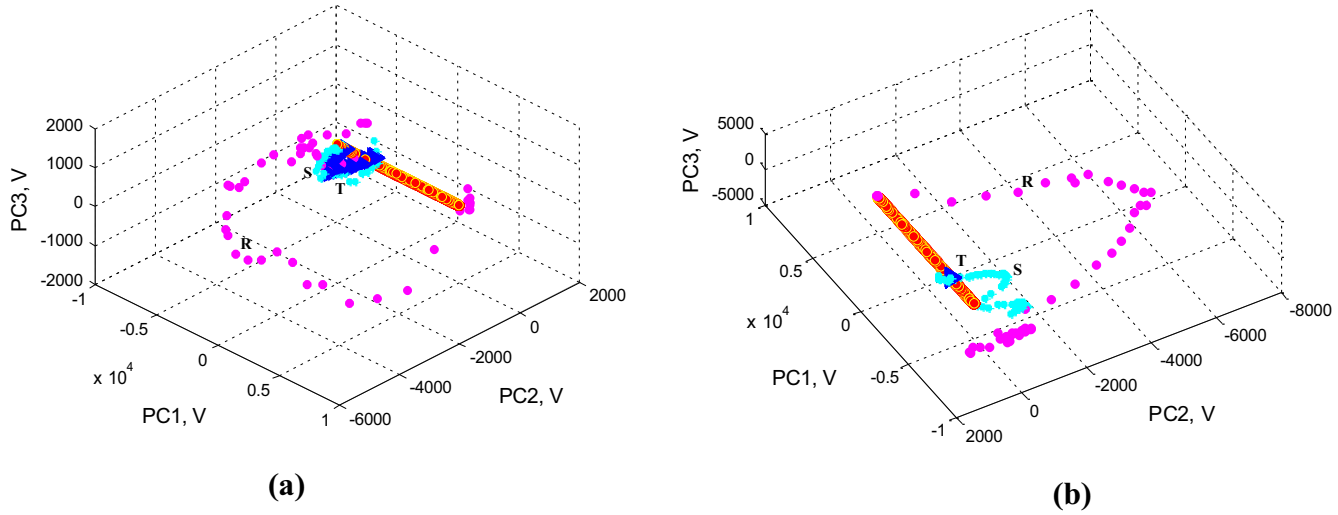

Fig. 16. Trajectories during lightning stroke (a) signal # 7; (b) signal # 9.

Table 6
EN of some testing lightning stroke signals.

Figure	Lightning type	Lightning current (kA)	EN		
			Phase R	Phase S	Phase T
Fig. 15		Ip = 6	2314	2923	15535
		Ip = 6, 5	2418	3018	15994
	Flash on live wires	Ip = 7, 5	2469	3062	16190
		Ip = 8.5	3416	4149	23842
		Ip = 10	3104	3746	21847
		Ip = 9	2764	3286	18538
Fig. 16a	Flash on transmission tower	Ip = 150	23301	5228	4257
		Ip = 160	26787	7287	4960
Fig. 16b		Ip = 200	27196	7678	133

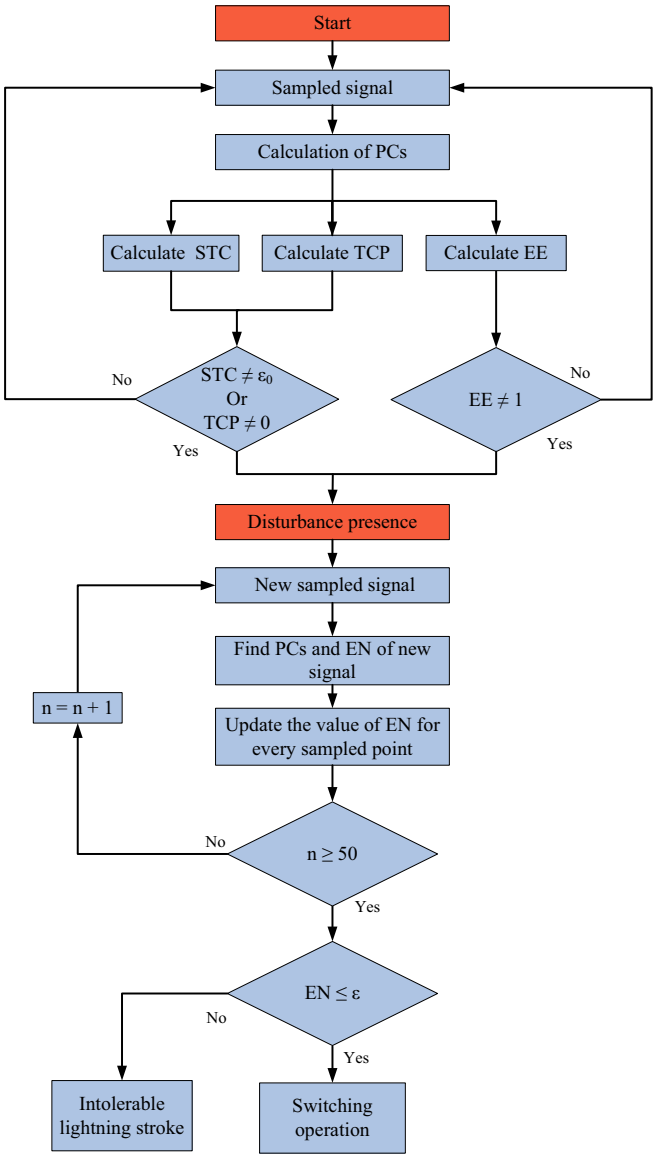

Fig. 17. Flow chart of detection and identification algorithms.

Euclidean Norm a switching operation or lightning stroke on the transmission line is identified.

Conclusions

In this paper a detection and identification algorithm is developed, which analysis the disturbed travelling waves considering a very short sampling rate. The algorithm is based on the Ellipsoidal Pattern (EP), which has three detection criteria, allowing a visual representation of the disturbance behavior.

This paper develops the switching operations and lightning strokes identification based on the Ellipsoidal Pattern and the Euclidean Norm. The algorithm performance is tested with different phenomena and shows acceptable success in identifying correctly disturbance and switching operations.

Acknowledgments

The authors gratefully acknowledge those contributions of the German Academic Interchange Program (DAAD), to the Institute of Electric Energy at the San Juan National University (IEE, UNSJ) and the Institute of Energy Systems, Energy Efficiency and Energy Economics (ie3) at the TU Dortmund University.

References

[1] EPRI AC Transmission Line Reference Book-200 kV and Above, 3rd ed. Electric Power Research Institute; December 2005.
[2] Adepitan JO, Oladiran EO. Analysis of the dependence of power outages on lightning events within the Ijebu province, Nigeria. J Environ Earth Sci 2012:850–6.
[3] Andersson G et al. Causes of the 2003 major grid blackouts in North America and Europe and recommended means to improve system dynamic performance. IEEE Trans Power Syst 2005;20(4):1922–8.
[4] North American Electric Reliability Corporation (NERC). 1992-2010. Events Analysis: System Disturbance Reports.
[5] Diendorfer G, Shulz W. Ground flash density and lightning exposure of power transmission lines. In: Power tech conference proceedings. Bologna: IEEE; 2003.
[6] Morales JA, Aguilar RP, Orduña EA, Pérez FE. Advances in lightning identification for transient based protection of power transmission lines. In: CLAGTEE. Ninth Latin-American congress on electricity generation and transmission, Argentina; November 2011.
[7] Zhengyou He et al. Study of a new method for power system transients classification based on wavelet entropy and neural network. Int J Electr Power Energy Syst 2011;33:402–10.
[8] Makarov YV, Reshetov VI, Stroev A, Voropai I. Blackout prevention in the United States, Europe, and Russia. Proc IEEE 2005;93(11):1942–55.
[9] Bompard Ettore, Huang Tao, Wu Yingjun, Cremenescu Mihai. Classification and trend analysis of threats origins to the security of power systems. Int J Elect Power Energy Syst 2013;50:50–64.
[10] ANSI/IEEE Standard 100. IEEE standard dictionary of electrical and electronics terms. 445 Hoes Lane, Piscataway, NJ 08854: IEEE Service Center.
[11] Nike S, Genci S, Marjela Q. Graphical method for estimating impact of distance line protection into electric power system stability. ATI-Appl Technol Innov 2010;1:9–20.
[12] IEEE PSRC WG D6. Power swing and out-of-step considerations on transmission lines; 2005. p. 1–59.
[13] Keokhoungning T, Premrudeepreechacharn S, Ngamsanroaj K. Evaluation of switching overvoltage in 500 kV transmission line interconnection Nam Theun 2 Power Plant to Roi Et 2 substation. In: Proc Asia pacific power and energy engineering conference; 2009. p. 1–4.
[14] Allan RN. Effects of protection systems operation and failures in composite system reliability evaluation. Int J Elect Power Energy Syst 1988;3:180–9.
[15] Johns AT, Salman SK. Digital protection for power system. IEEE power series 15. Peter Peregrinus Ltd.; 1995.

[16] Rebizant W et al. Digital signal processing in power system protection and control, signals and communication technology. London: Springer-Verlag; 2011.
[17] Granados R, Romero R, Osornio RA, Garcia A, Cabral E. Techniques and methodologies for power quality analysis and disturbances classification in power systems: a review. IET Gener Transm Distrib 2011;5:519–29.
[18] Flores RA. State of the art in the classification of power quality events, an overview. In: Proc 10th int conf harmonics quality of power, vol. 1; 2002. p. 17–20.
[19] Manish K, Rajiv K. Classification of power quality events – a review. Int J Elect Power Energy Syst 2012;43:11–9.
[20] Santoso S, Grady WM, Powers EJ, Lamore J, Bhatt SC. Characterization of distribution power quality events with Fourier and wavelet transforms. IEEE Trans Power Del 2000;15(1):247–54.
[21] Masoum M, Jamali S, Ghaffarzadeh N. Detection and classification of power quality disturbances using discrete wavelet transform and wavelet networks. IET Sci Meas Technol 2010;4(4):193–205.
[22] Tong W, Song X, Lin J, Zhao Z. Detection and classification of power quality disturbances based on wavelet packet decomposition and support vector machines. In: Proc ISCP, vol. 4; 2006.
[23] Wang M et al. Disturbance identification method for lightning wave invading grid. In: Proc DRPT; 2011. p. 1825–9.
[24] Elango MK, Kumar AN, Duraiswamy K. Identification of power quality disturbances using Artificial Neural Networks. In: Proc ICPS; 2011. p. 1–6.
[25] Dash PK, Biswal M. Measurement and classification of simultaneous power signal patterns with an S-transform variant and Fuzzy Decision Tree. IEEE Trans 2012.
[26] Mahmood F, Qureshi SA, Kamran M. Application of wavelet multi-resolution analysis & perceptron neural networks for classification of transients on transmission line. In: Proc IEEE int conf on power engineering; 2008. p. 1–5.
[27] Lopes FV, Fernandes D, Neves WLA. Transients detection in EHV transmission lines using park's transformation. In: Proc IEEE int conf transmission and distribution; 2012. p. 1–6.
[28] Costa FB et al. A tool for fault and power quality disturbance analysis in oscillographic records. In: Proceedings of the 2011 3rd international youth conference; 2011. p. 1–6.
[29] Costa FB, Souza BA, Brito NSD. Real-time detection of fault-induced transients in transmission lines. Electron Lett 2010;46:753–5.
[30] Dubey R, Samantaray SR. Wavelet singular entropy-based symmetrical fault-detection and out-of-step protection during power swing. IET Gener Transm Distrib 2013;7:1123–34.
[31] Panigrahi BK, Pandi VR. Optimal feature selection for classification of power quality disturbances using wavelet packet-based fuzzy k-nearest neighbors algorithm. IET Gener Transm Distrib 2009;3:296–306.
[32] Naik Chirag A, Kundu Prasanta. Power quality index based on discrete wavelet transform. Int J Elect Power Energy Syst 2013;53:994–1002.
[33] Ribeiro H, Marques H, Borges BV. Characterizing and monitoring voltage transients as problem to sensitive loads. Int J Electr Power Energy Syst 2012;43:1305–17.
[34] Ghaemi AH, Askarian Abyaneh H, Mazlumi K. Harmonic indices assessment by wavelet transform. Int J Electr Power Energy Syst 2011;33:1399–409.
[35] Erişti H, Yıldırım Ö, Erişti B, Demir Y. Optimal feature selection for classification of the power quality events using wavelet transform and least squares support vector machines. Int J Electr Power Energy Syst 2013;49:95–103.
[36] Abdelsalam Abdelazeem A, Eldesouky Azza A, Sallam Abdelhay A. Classification of power system disturbances using linear Kalman filter and fuzzy-expert system. Int J Electr Power Energy Syst 2012;43:688–95.
[37] Kaewarsa S, Attakitmongcol K, Kulworawanichpong T. Recognition of power quality events by using multiwavelet-based neural networks. Int J Electr Power Energy Syst 2008;30:254–60.
[38] Oleskovicz M et al. Power quality analysis applying a hybrid methodology with wavelet transforms and neural networks. Int J Electr Power Energy Syst 2009;31:206–12.
[39] Lobos T et al. Application of wavelets and Prony method for disturbance detection in fixed speed wind farms. Int J Electr Power Energy Syst 2009;31:429–36.
[40] Gencer Ö, Öztürk S, Erfidan T. A new approach to voltage sag detection based on wavelet transform. Int J Electr Power Energy Syst 2010;32:133–40.
[41] Xiao X, Xu F, Yang H. Short duration disturbance classifying based on S-transform maximum similarity. Int J Electr Power Energy Syst 2009;31:374–8.
[42] Suja S, Suja Jovitha. Pattern recognition of power signal disturbances using S transform and TT transform. Int J Electr Power Energy Syst 2010;32(1):37–53.
[43] Diaz HN, Castro M. Aplicación de la transformada wavelet en los sistemas eléctricos de potencia. Casilla 6-D, Arica-Chile: Universidad de Tarapaca.
[44] Morales JA, Orduña EA, Rehtanz C, Cabral RJ, Bretas AS. Comparison between PCA and WT filtering methods for lightning stroke classification on transmission lines. In: Proc SIPDA; October 2013 [in press].
[45] Wang F. On power quality and protection. Goteborg (Sweden): Chalmers University of Technology; 2001.
[46] Jollife I. Principal component analysis. New York: Springer-Verlag; 1986.
[47] ATP DRAW version 3.5 for Windows 9x/NT/2000/XP Users'Manual.
[48] Heidler F, Cvetic M, Stanic BV. Calculation of lightning current parameters. IEEE Trans Power Deliv 1999(14):399–404.
[49] Martínez JA, Castro-Aranda F. Lightning performance analysis of overhead transmission lines using the EMTP. IEEE Trans Power Deliv 2005;20(3):2200–10.
[50] CIGRE working group 13.05. The calculation of switching surges (I). A comparison of transient network analyzer results. Electra, vol. 19; 1971. p. 67–78.
[51] CIGRE working group 13-02 switching surges phenomena in EHV systems. Switching overvoltages in EHV and UHV systems with special reference to closing and re-closing transmission lines. Electra, 30; 1973. p. 70–122.
[52] CIGRE working group 33.02. Guidelines for representation of network elements when calculating transients. Paris; 1990.
[53] IEEE working group 15.08.09. Modeling and analysis of system transients using digital programs. Piscataway: IEEE PES Special Publication 99TP-133-0, IEEE Operations Center; 1998.
[54] Hart J. Distance to an ellipsoid. In: Heckbert Paul, editor. Graphics gems IV. New York NY: Academic Press, Inc.; 1994. p. 113–9.
[55] Texas Instruments. "Floating-point digital signal processor Tms320c6713". SPRS 186L, Dallas, Texas; November 2005.
[56] Texas instruments. "User's Guide, Ads8364evm". Dallas, Texas; 2002.